Physicochem. Probl. Miner. Process., 55(1), 2019, 301-310

http://www.journalssystem.com/ppmp

Physicochemical Problems of Mineral Processing

ISSN 1643-1049

Received March 30, 2018; reviewed; accepted May 9, 2018

Adsorption behavior and mechanism of an ether amine collector on collophane and quartz

Ji Fang [1], Yingyong Ge [1, 2], Jun Yu [3]

[1] School of Resources and Environmental Engineering, Wuhan University of Technology, Wuhan 430070, China;

[2] Hubei Key Laboratory of Mineral Resources Processing & Environment, Wuhan 430070, China;

[3] China BlueStar Changsha Design and Research Institute, Changsha 410016, China

Corresponding author: fangji1993@foxmail.com (Ji Fang)

Abstract: The adsorption behaviors of an ether amine surfactant, N1-(3-((8-methyl-nonyl)oxy) propyl)propane-1,3-diamine, on collophane and quartz were studied. Batch adsorption experiments were conducted to characterize the thermodynamic behavior of the adsorption process and to calculate the maximum adsorption. Results demonstrated that the adsorption of the ether amine on quartz was greater than collophane. Adsorption mechanisms were studied by means of contact angle measurement, zeta potential measurement, FT-IR analysis, and X-ray photoelectron spectroscopy. The results showed that the adsorption of the ether amine surfactant on quartz surface was easier and more efficient than collophane. Micro-flotation tests testified that the collector can efficiently separate collophane from quartz at room temperature in neutral medium.

Keywords: adsorption, collophane, collector, ether amine surfactant, flotation

1. Introduction

Phosphate ore, a vital non-renewable resource, is greatly important for agriculture industry (Santana et al., 2008). It is reported that fertilizer industry consumes more than 95% of phosphate ore all over the world (Santana et al., 2012). Due to the depletion of high quality phosphate ores, the shortage of phosphorus may become a potential threat for the development of agriculture and phosphorus-based chemicals. In this context, the technique of recovering phosphate from low-grade ores, such as siliceous–calcareous collophane, is becoming more and more important. Quartz, dolomite are the common gangue minerals in collophanite ore (Zhou et al., 2015). Meanwhile, due to the similar surface characters among these three minerals, it is very difficult to separate collophane from quartz (Abouzeid et al., 2009).

At present, flotation is the most widely used technique to concentrate collophane from siliceous phosphate ore. More than half of worldwide production of commercial phosphate is upgraded by flotation (Boulos et al., 2014). In the process of flotation, collector plays a vitally important role and it is indeed significant to choose an efficient collector (Li et al., 2017; Sahoo et al., 2015). Lots of research, relative to the flotation technique and flotation reagents toward the separation of collophane from gangue minerals, have been reported (Ahmed et al., 2014; Mariana et al., 2012; Yu et al., 2016; Wang et al., 2006). There are some apparent drawbacks of conventional collectors used in phosphate ore flotation processing, such as poor solubility and poor selectivity at room temperature. Therefore, exploring high selectivity and temperature-insensitive collectors is an efficient way to solve this problem.

The excellent collecting performance of the amine surfactants, usually used as novel collectors, have been reported many times (Liu et al., 2016; Hanna, 1975). Furthermore, Salah et al. conducted a comparison study to anionic and cationic collectors in flotation of a siliceous phosphate rock, the results show that amine collectors obtained a better metallurgical performance relative to sodium oleate (Salah et al., 2011). Hence, there is an important significance to study the application of amine surfactants to

DOI: 10.5277/ppmp18132

concentrate collophane from gangue minerals, especially quartz.

Aim of the present study is to respectively investigate the adsorption behavior of a kind of ether amine surfactant (EA), a novel cationic collector, on collophane and quartz. The effect of the ether amine surfactant on separating collophane from quartz was evaluated. The mechanism of adsorption behavior was interpreted by means of X-ray photoelectron spectroscopy, zeta potential measurements, contact angle measurements and FTIR spectra analysis. Flotation tests were conducted to estimate the flotation performance of the ether amine collector.

2. Experimental

2.1. Materials

High purity samples of collophane and quartz in this study were obtained from Hubei Province, China. The pure minerals were crushed and ground to -37 μm in ceramic ball mill. The chemical composition of each purity sample was confirmed by X-ray fluorescence spectroscopy (XRF) and the results were given in Table 1. Chemical analysis results indicated that the purities of collophane and quartz were more than 95%. The specific surface areas of collophane and quartz determined by the BET test were presented in Table 2.

Table 1. Chemical analysis results of collophane and quartz (mass fraction, %)

sample	chemical composition								
collophane	CaO	MgO	Al_2O_3	SiO_2	SrO	P_2O_5	Fe_2O_3	F	LOI
	56.62	0.08	0.05	4.20	0.04	39.56	1.69	1.12	0.58
quartz	SiO_2	Al_2O_3	P_2O_5	CaO	Fe_2O_3	Cl	LOI		
	99.67	0.071	0.053	0.056	0.011	0.011	0.13		

(LOI=Loss on ignition)

Table 2. Specific surface of collophane and quartz

Particle Size (μm)	Collophane(m^2/g)	Quartz(m^2/g)
-37	2.8666	0.3156

N1-(3-((8-methyl-nonyl)oxy) propyl)propane-1,3-diamine, $C_{16}H_{36}ON_2$, an ether amine surfactant, with technical purity was obtained from Baling petrochemical co. LTD, China. There were two amidogens and one ether linkage in the amine molecule. Therefore, the ether amine surfactant was named EA in this paper.

Solutions of HCl and NaOH were used to adjust the pH. Meanwhile, distilled water was used for adsorption experiment.

2.2. Adsorption experiments

Batch adsorption experiments were conducted to characterize thermodynamic behaviors of the adsorption process and to calculate the maximum adsorption. The amount of surfactant adsorbed on each mineral surface was measured by the solution depletion method using a UV-VIS spectrophotometer (UV775B, China). Pure mineral sample was immersed in the surfactant solution with different concentrations. Then, adsorption experiments were performed in the water-bathing constant temperature vibrator for 1h. The surfactant adsorption on each mineral surface was calculated using a mass balance by Eq. (1). The maximum adsorption capacity was determined by the Langmuir isotherm Eq. (2) (Falil et al., 2016):

$$q_e = \frac{(C_0 - C_e)\mathrm{v}}{\mathrm{mA}} \tag{1}$$

$$\frac{C_e}{q_e} = \frac{1}{K_l q_m} + \frac{C_e}{q_m} \tag{2}$$

$$lnq_e = \ln K_f + \frac{\ln C_e}{\mathrm{n}} \tag{3}$$

where q_e and q_m (mol/m^2) were respectively the equilibrium adsorption value and the maximum

adsorption value, C_0 and C_e were respectively the initial concentrations and the equilibrium concentrations of EA (mol/dm^3), V was volume of the solution (cm^3), and m (g) was the mass of mineral sample for each test, A was the specific surface area (m^2/g) of mineral particle, and K_l was the Langmuir constant related to the energy or net enthalpy of adsorption, K_f was the Freundlich constant.

2.3. Contact angle measurements

The contact angle of collophane and quartz before and after treatment with EA were measured using Kruss K100 instrument (KRüSS, Hamburg, Germany). The pure mineral samples were immersed in distilled water or EA solution at different pH values for 5 min, respectively. After drying (333 K)， pure mineral samples were pressed to round tablets (d=1 cm). Finally, the contact angle measurements were performed.

2.4. Zeta potential measurements

The zeta potentials were measured using a Malvern Zetasizer Nano ZS90 instrument (Made in England). The zeta potentials of minerals in distill water and in EA solution were compared in different pH value, and the pH value of the suspension was adjusted to a desired value using HCl or NaOH solution. The concentration of the mineral suspension was 0.04 wt%. The measurements were conducted at room temperature (298 K). The average zeta potential values of at least three independent measurements were recorded with a measurement error of ±2 mV.

2.5. FT-IR measurements

Fourier Transform Infrared (FTIR) spectra ranging from 4000 to 500 cm^{-1} was used to characterize EA and its adsorption on the different mineral surfaces at room temperature. After further grounding in an agate mortar, the mineral pellets were prepared by mixing KBr (optically pure) and mineral at the mass ratio of 200/1. The spectra of the samples were obtained by a Fourier transform infrared spectrometer Nicolet.

2.6. X-ray photoelectron spectroscopy

X-ray photoelectron spectroscopy (XPS) measurements were performed in an ultrahigh vacuum VG Multilab 2000 electron spectrometer equipped with a multichannel detector. The spectra were excited using Al Ka radiation. XPS spectrogram of minerals before and after reacting with EA were obtained, respectively.

2.7. Micro-flotation tests

Flotation tests were carried out in a XFGC-80 flotation machine with a 100 cm^3 cell and using the ether amine surfactant (EA) as the collector. The mineral suspension was prepared by adding 5.0 g of quartz or collophane to 100 cm^3 of solutions in the micro-flotation test. The suspension was agitated with a rotational speed of 2000 rpm. After agitating for 3 min, the pH value of suspension was adjusted to a desired value with the addition of HCl or NaOH solutions. Keep agitating for 5 min before adding collector in mineral suspension. After introduction of collector, the suspension was conditioned for 5 min. Subsequently, the foam product was collected, dried and weighed in each test. The recovery was calculated based on the dry weights of the products obtained. Each test was repeated three times. The average recovery of three flotation experimental results was reported.

3. Results and discussion

3.1. Adsorption experiments

3.1.1. Adsorption behavior of EA

The adsorption measurements of EA on the surfaces of collophane and quartz as a function of EA concentration were performed in neutral medium (pH=7.5). Figure. 2 showed the adsorption isotherms of EA on collophane and quartz surfaces at three different temperatures, respectively. The results

indicated that the adsorption quantity of EA on the mineral surface increased with the increasing concentration of EA for the both minerals. Apparently, the adsorption quantity on the quartz surface was greatly higher than on collophane surface, especially under room temperature. Meanwhile, for collophane, the adsorption quantity of EA increased with the increasing of temperature. On the contrary, the adsorption quantity of EA on quartz surface decreased with the increase of temperature. It suggested that the surfactant might be used as collector to concentrate collophane via removing quartz with reverse flotation at a low collector dosage and at room temperature.

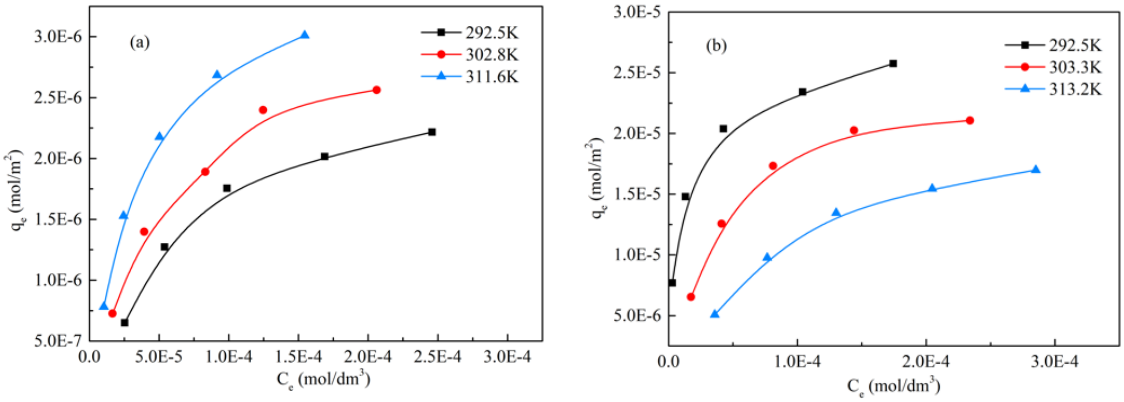

Fig. 1. Adsorption isotherms of EA onto mineral surfaces (a - collophane; b - quartz)

Table 3. Isotherm parameters for the adsorption gained from Langmuir and Freundlich models

mineral	T (K)	Langmuir			Freundlich		
		q_m (mol/m^2)	K_L	R^2	n	K_F	R^2
collophane	292.5	2.95×10^{-6}	12940.89	0.9918	1.89	2.00×10^{-4}	0.9075
	302.8	3.31×10^{-6}	17675.29	0.9914	1.97	2.14×10^{-4}	0.9435
	311.6	3.74×10^{-6}	27068.37	0.9992	2.02	2.63×10^{-4}	0.9358
quartz	292.5	2.69×10^{-5}	92257.74	0.9966	3.46	3.39×10^{-4}	0.9461
	303.3	2.54×10^{-5}	23195.71	0.9935	2.21	1.07×10^{-3}	0.8905
	313.2	2.49×10^{-5}	7996.38	0.9826	1.72	2.14×10^{-3}	0.9336

Langmuir and Freundlich adsorption isothermal adsorption model, as shown in Eq. (2) and Eq. (3), respectively, were used to calculate the maximum adsorption value of EA on each mineral surface, and the results were showed in Table 3. It was easy to know that Langmuir adsorption isothermal adsorption model was more appropriate to describe adsorption behavior. As shown in Table 3, at the condition of room temperature (292.5 K), the maximum adsorption value of EA on quartz was 2.69×10^{-5} mol/m^2, more than 9 times greater than on collophane. We may safely draw the conclusion that the adsorption of EA on quartz surface was easier and more efficient than collophane.

3.1.2 Thermodynamic calculation

Langmuir adsorption isotherm model was used to evaluate the equilibrium of adsorption process. At infinite dilute solution, i.e. adsorbate concentration in the solution tends to zero, the values of activity coefficients approach unity and the definition of k_0 is simplified to Eq.(4) and Eq.(5) (Nguyen et al., 2014):

$$k_D = \frac{q_e}{C_e} \tag{4}$$

$$lnk_0 = \lim_{C_e \to 0} lnk_D \tag{5}$$

Having calculated the k_0, the thermodynamics parameters, the standard Gibbs free energy change (ΔG_0) (kJ/mol), the standard enthalpy change (ΔH_0) (kJ/mol) and the standard entropy change (ΔS_0) (J/mol K) can be estimated as Eq. (6) (Monfared et al., 2015; Manasi and Rajesh, 2014):

$$lnk_0 = \frac{-\Delta G^0}{\mathrm{RT}} = \frac{\Delta S^0}{R} - \frac{\Delta H^0}{RT} \tag{6}$$

where q_e is the amount of EA adsorption at the equilibrium per unit mass of adsorbent (mg/g), C_e is the solution equilibrium concentration (mg/cm^3), R is a constant, T is the temperature in Kelvin.

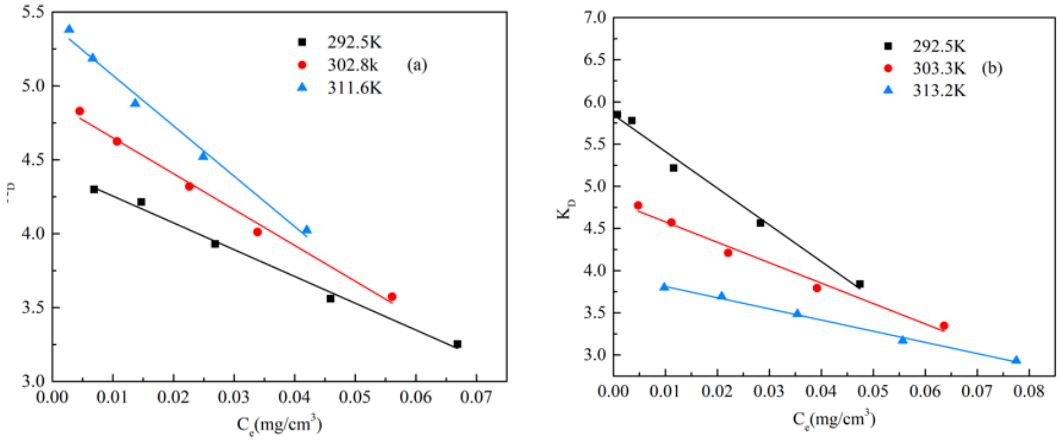

Fig. 2. Linear plots of (k_D) versus (C_e) (a-collophane, b-quartz)

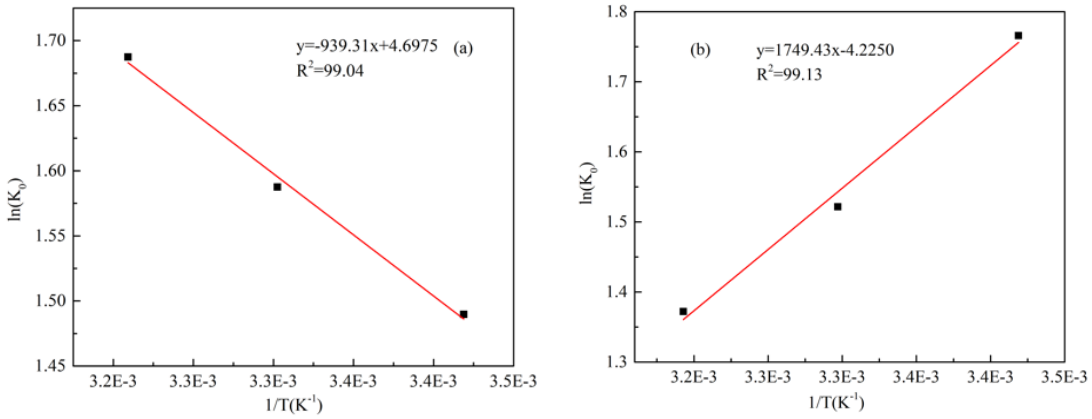

Fig. 3. Linear plot of ln(k_0) versus ($1/T$) for estimation of the thermodynamics parameter (a-collophane, b-quartz)

Based on adsorption experiments and Langmuir adsorption isotherm model, the fitting curves of isothermal adsorption were shown as Fig. 2, respectively, under different adsorption temperatures. Subsequently, the value of k0 for corresponding temperature can be found from the intercept of the resulting straight line. Then, linear plots of ln(k_0) versus ($1/T$) for estimation of the thermodynamics parameter were shown as Fig. 3. Meanwhile, ΔG_0 was calculated by the values of k_0 in different temperatures.

Finally, ΔH_0 and ΔS_0 of the adsorption equilibrium can be obtained from the slope and intercept of the curves in the plot of the ln(k_0) versus ($1/T$). All of the thermodynamics parameter was obtained and shown in Table 4.

Table 4. Thermodynamic parameters for the adsorption at different temperatures

mineral	T (K)	ΔG^0 (kJ/mol)	ΔH^0 (kJ/mol)	ΔS^0 (J·mol^{-1}·K^{-1})
collophane	292.5	-3.62	7.81	39.04
	302.8	-3.99		
	311.6	-4.37		
quartz	292.5	-4.29	-14.54	-35.11
	303.3	-3.83		
	313.2	-3.57		

As shown in Table 4, the negative values of ΔG_0 suggested that the adsorption of EA onto each mineral surface was spontaneous. Different with collophane, the adsorption of EA onto quartz was less spontaneous at higher temperatures due to reducing of the value of ΔG_0 with the temperature increase. For a physical sorption, the change in the value of free energy was supposed to be in the range of -20~0 kJ/mol (Monfared et al., 2015). Here, all of the free energy changes(ΔG_0) was less than -20 kJ/mol where physical or electrostatic adsorption was expected to be the prevailing mechanism.

Compared with collophane, the standard enthalpy change (ΔH_0) of quartz was negative. The negative ΔH_0 value indicated that the adsorption of EA on quartz was an exothermic process. It was reported that bonding strengths lower than 84 kJ/mol were typically considered as those of physisorption bonds (Falil et al., 2016). Therefore, the small value of ΔH_0 was further confirming the physical characteristic of the adsorption process.

According to the thermodynamic calculation, the separation of collophane from quartz could be facilitated at lower temperature, because of the exothermic character of adsorption onto quartz and the endothermic character of onto collophane.

3.2. Adsorption mechanism of EA

3.2.1. Contact angle measurements

Fig. 4 showed the effect caused by EA in the contact angle measurements of collophane and quartz as a function of EA concentration. Before interaction with EA, both minerals were hydrophilic. Furthermore, collophane were greater hydrophilic with the contact angle about 20°.

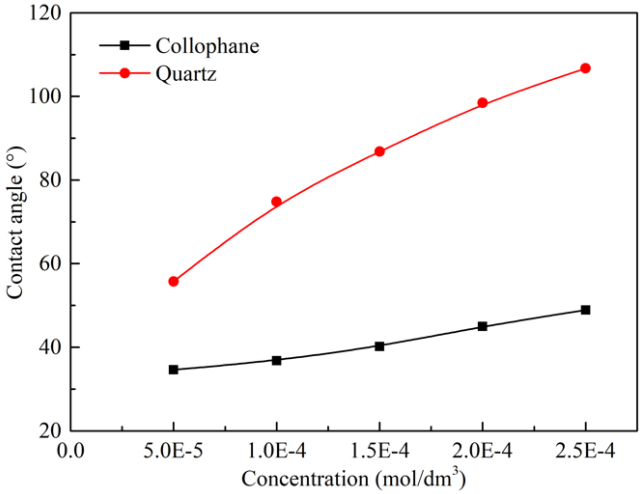

Fig. 4. Contact angle of minerals as a function of EA concentration

After EA interacting with the mineral surfaces, respectively, the increase of contact angle can be observed. What's more, the insignificant increase of contact angle for collophane was observed. Compared with quartz, the increase of collophane contact angle was very slight. Therefore, the interaction between EA and quartz was greatly stronger than collophane. The change observed in the measurements of each mineral contact angle after the interaction with EA could be related to the adsorption of EA molecule onto the mineral surfaces. Likewise, the contact angle measurements indicated a higher adsorption of EA molecule at quartz surface.

3.2.2 Zeta potential measurements

The zeta potential results of minerals in distilled water and EA solutions at different pH values were given in Fig. 5. The isoelectric point (IEP) was determined from the pH value at which the reversal of charge from positive to negative occurred. As shown in Fig. 5, the zeta potential of collophane in distill water was negative and decreased with the increase of the pH value, and the IEP of quartz was approximately 2.4 mV.

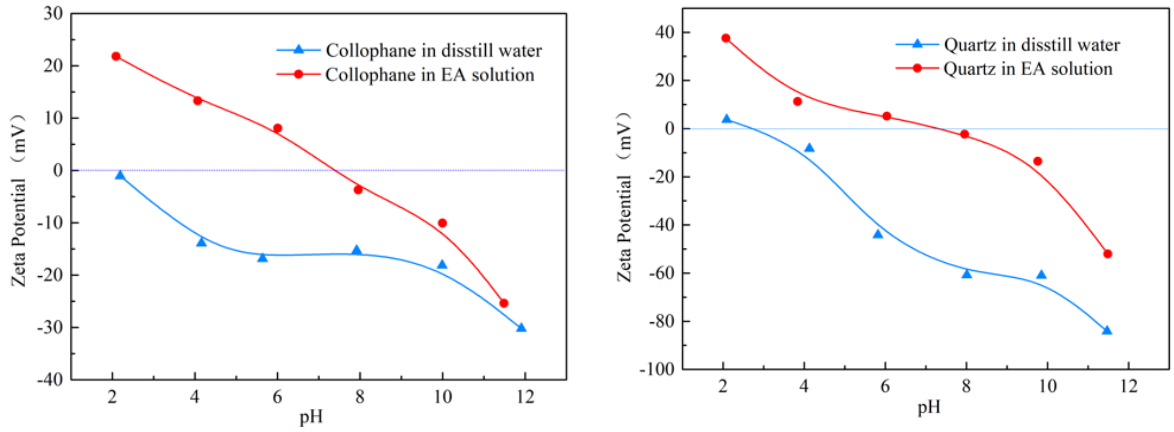

Fig. 5. Zeta potential of minerals in distilled water and EA solution

Nevertheless, as shown in Fig. 5, compared with in distilled water, zeta potential of both minerals greatly increased in EA solution. The IEP of collophane and quartz increased to 7.5 and 7.2, respectively. Furthermore, the significant increase of zeta potential of collophane appeared in pH=2~7 related to the favorable adsorption of EA. Therefore, the most appropriate pH value range for the adsorption of EA on collophane was 2~6. Similarly, the appropriate pH value range for the adsorption on quartz was 6~10. It can be predicted that the appropriate pH value range for separating quartz from collophane were 6 to 10.

The observed changes in zeta potential values for both minerals after interaction with EA could attribute to the adsorption of EA on the mineral surfaces. And the difference of appropriate pH value range for adsorption made a great potentiality to separate collophane from quartz via using EA as collector.

3.2.3. FT-IR analysis

In order to investigate the adsorption mechanism of EA on the mineral surfaces, the raw minerals and minerals reacting with EA were characterized by infrared spectrometry.

The FTIR spectra of collophane before and after reacting with EA was shown in Fig. 6a. After reacting with EA, the adsorption of EA on collophane surface was too few to make new characteristic peaks appear. Figure. 6b displayed the infrared spectra of quartz before and after reacting with EA. Compared with the infrared spectra of pure quartz, two new characteristic peaks appear at 2921cm^{-1} and 2853cm^{-1} due to the stretching vibration of -CH2 in EA molecules adsorbed on quartz surface. It can be concluded that EA molecules adsorbed on quartz surface.

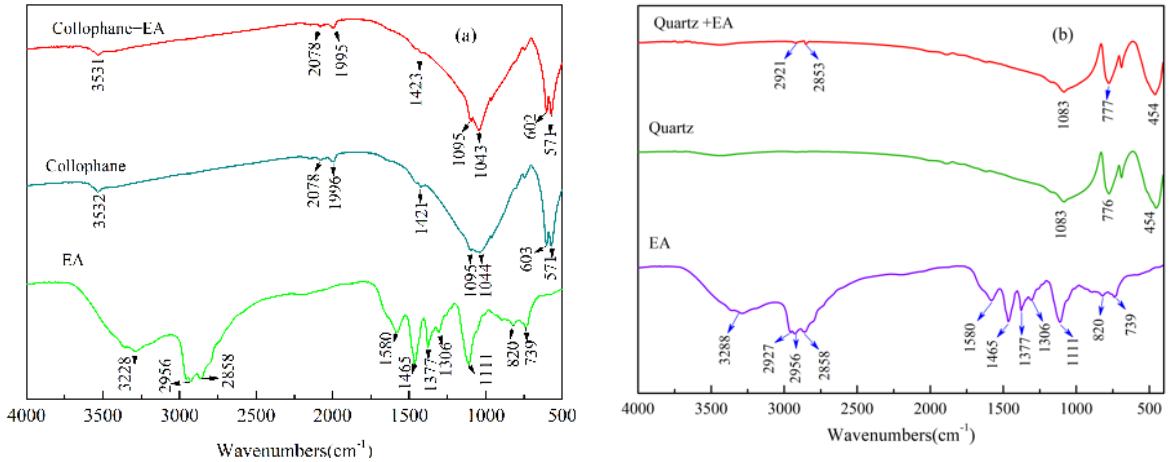

Fig. 6. FTIR spectra of minerals before and after reacting with EA

3.2.4. XPS analysis

XPS measurements of the mineral surfaces after adsorption experiments were carried out to analyze the adsorption behaviors. Changes in the elemental species detected on the mineral surfaces were investigated by XPS to identify which species were present after adsorption and to compare with untreated minerals (Nguyen et al., 2014).

The results of elements scan on mineral surfaces before and after adsorption were shown as Fig. 7. The binding energy for each element was shown in Table 5. Based on the binding energies, the relative contents of each element on mineral surfaces were calculated and shown in Table 6.

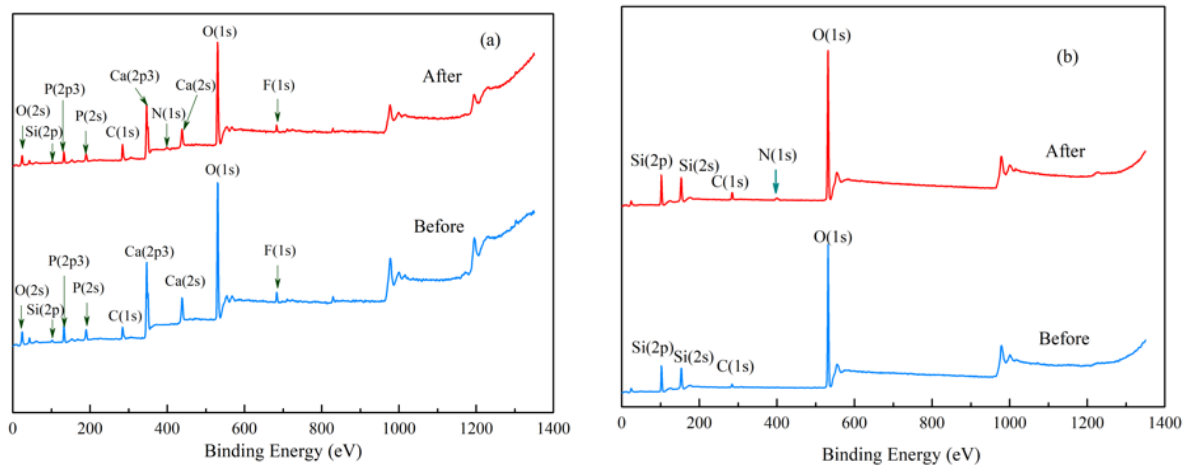

Fig. 7. XPS spectrogram of minerals before and after reacting with EA (a-collophane, b-quartz)

Table 5. Relative concentration of surface elements on minerals before and after reacting with EA

mineral	element	relative concentration（%）		change（%）
		before	after	
collophane	O1s	55.25	50.85	-4.40
	Ca2p	15.70	14.07	-1.63
	P2p	10.03	9.99	-0.04
	C1s	14.32	20.07	5.75
	F1s	3.23	3.38	0.15
	Si2p	1.47	0.79	-0.68
	N1s	0.00	0.85	0.85
quartz	Si2p	29.43	28.20	-1.23
	O1s	64.63	58.15	-6.48
	C1s	5.94	11.81	5.87
	N1s	0.00	1.84	1.84

As shown in Fig. 7, after reacting with EA, the N1s spectrum which was the characteristic peak of amine surfactant (EA) appeared in each mineral XPS photoelectron spectra. It showed that EA molecule adsorbed on minerals surface. The changes of relative concentration of surface elements on minerals before and after reacting with EA were shown in Table 5. According to Table 5, the increase of relative concentrations of C and N indicated that EA molecule adsorbed on mineral surfaces. At the same time, the relative concentrations of other elements declined in different degree. It was due to the coverage of EA molecule on mineral surfaces. Besides, comparing the relative concentrations of N on collophane and quartz surfaces, the increase rate of the relative concentrations of N on quartz surface (1.84%) was larger than on collophane (0.85%). This indicated that the interaction between EA and quartz surface was greater than collophane surface. The result was consistent with the results of adsorption experiments and contact angle measurements.

3.3. Micro-flotation tests

The flotation recovery of collophane and quartz as a function of pH value under 2×10^{-5} mol/dm^3 EA (298 K) was listed in Fig. 8. The result showed that the amine surfactant (EA) exhibited stronger collecting power to quartz than to collophane, and the preferable pH values for separating quartz from collophane were 6 to 10. Obviously, the best pH value was 8. The effect of initial EA concentration on flotation recovery of collophane and quartz at pH 8 was showed in Fig. 9. The result indicated that with increasing dosage of EA, the flotation recovery of collophane and quartz increased. When the initial concentration of EA was greater than 2×10^{-5} mol/dm^3, the flotation recovery of quartz increased slowly.

The results of micro-flotation tests demonstrated that EA exhibited good flotation performances to quartz and might be used as a collector for separating collophane and quartz with reverse flotation technology at room temperature in neutral medium.

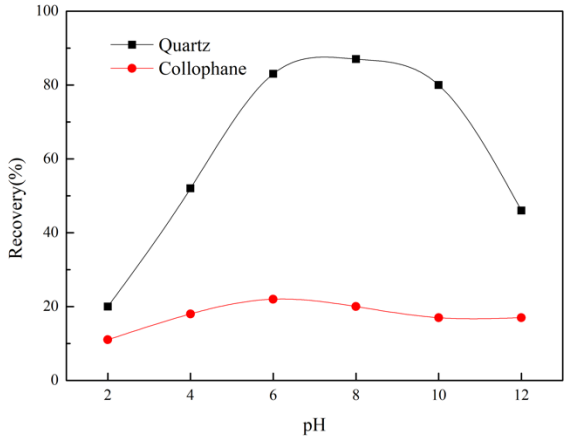

Fig. 8. Recovery of collophane and quartz as a function of pH value

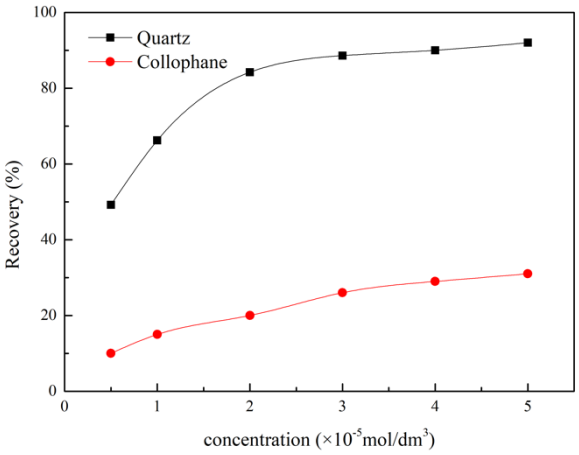

Fig. 9. Recovery of collophane and quartz as a function of initial EA concentration

4. Conclusions

Adsorption experiments showed that the adsorption of the ether amine collector (EA) on quartz surface was easier and more efficient than collophane. The maximum absorptive capacity of EA on quartz was more than 9 times greater than on collophane. Due to the exothermic character of the adsorption onto quartz and the endothermic character of collophane, lower temperature could facilitate the separation of collophane from quartz. Adsorption mechanism analysis results showed that the adsorptions of EA on both quartz and collophane were physical adsorption.

Micro-flotation tests testified that the ether amine collector (EA) have stronger collecting power to quartz than collophane, and the preferable pH values for separating quartz from collophane were 6 to 10. As a novel cationic collector, the ether amine surfactant exhibited a good performance in the flotation

separation of collophane from quartz at room temperature in neutral medium.

Acknowledgements

The authors acknowledge the support of the National Natural Science Foundation of China (Grant Nos.51554288).

References

ABOUZEID, A. Z. M., NEGM, A. T., ELGILLANI, D. A., 2009. *Upgrading of calcareous phosphate ores by flotation: effect of ore characteristics*, International Journal of Mineral Processing, 90(1-4), 81-89.

AHMED, H. A. M., 2014. *Flotation after a direct contact of flotation reagents with carbonate particles – part 2: phosphate ore*, Physicochemical Problems of Mineral Processing, 49(2), 713-723.

BOULOS, T. R., YEHIA, A., IBRAHIM, S. S., & YASSIN, K. E., 2014. *A modification in the flotation process of a calcareous–siliceous phosphorite that might improve the process economics*, Minerals Engineering, 69(3), 97-101.

FALIL, F., ALLAM, F., GOURICH, B., VIAL, C., AUDONNET, F., 2016. *Adsorption of astrazon orange g onto natural moroccan phosphate rock: a mechanistic study*, Journal of Environmental Chemical Engineering, 4(2), 2556-2564.

HANNA, H. S., 1975, *The role of cationic surfactants in the selective flotation of phosphate ore constituents*, Powder Technology, 12(1), 57-64.

LI, X., ZHANG, Q., HOU, B., YE, J., MAO, S., LI, X., 2017. *Flotation separation of quartz from collophane using an amine collector and its adsorption mechanisms*, Powder Technology 318, 224-229.

LIU, W., LIU, W., WANG, X., WEI, D., ZHANG, H., LIU, W., 2016. *Effect of butanol on flotation separation of quartz from hematite with n-dodecyl ethylenediamine*, International Journal of Mining Science and Technology, 26(6), 1059-1063.

MANASI., RAJESH, V., RAJESH, N., 2014. *Adsorption isotherms, kinetics and thermodynamic studies towards understanding the interaction between a microbe immobilized polysaccharide matrix and lead*, Chemical Engineering Journal, 248, 342-351.

MARIANA, A., DOS, SANTOS., RICARDO C., SANTANA, FABIANO CAPPONI., CARLOS H., ALTAIDE., MARCOS A. S. BARROZO., 2012. *Influence of the water composition on the selectivity of apatite flotation*, Separation Science & Technology, 47(4), 606-612.

MONFARED, A. D., GHAZANFARI, M. H., JAMIALAHMADI, M., HELALIZADEH, A., 2015. *Adsorption of silica nanoparticles onto calcite: equilibrium, kinetic, thermodynamic and DLVO analysis*, Chemical Engineering Journal, 281, 334-344.

NGUYEN, A. V., PLACKOWSKI, C., BRUCKARD, W. J., 2014. *Surface characterisation, collector adsorption and flotation response of enargite in a redox potential controlled environment*, Minerals Engineering, 65(6), 61-73.

SAHOO, H., RATH, S. S., JENA, S. K., MISHRA, B. K., DAS, B., 2015. *Aliquat-336 as a novel collector for quartz flotation*, Advanced Powder Technology, 26(2), 511-518.

SALAH, A. T., ROE-HOAN, Y., DONGCHEOL, S., 2011. *A comparison of anionic and cationic flotation of a siliceous phosphate rock in a column flotation cell*, International Journal of Mining Science and Technology, 21(1), 147-151.

SANTANA, R. C., FARNESE, A. C. C., FORTES, M. C. B., ATAIDE, C. H., BARROZO, M. A. S., 2008. *Influence of particle size and reagent dosage on the performance of apatite flotation*, Separation & Purification Technology, 64(1), 8-15.

SANTANA, R. C., FARNESE, A. C. C., FORTES, M. C. B., ATAIDE, C. H., BARROZO, M. A. S., 2012. *Flotation of fine apatite ore using microbubbles*, Separation & Purification Technology, 98(39), 402-409.

WANG, X., NGUYEN, A. V., MILLER, J. D., 2006. *Selective attachment and spreading of hydroxamic acid–alcohol collector mixtures in phosphate flotation*, International Journal of Mineral Processing, 78(2), 122-130.

YU, J., GE, Y., HOU, J., 2016. *Behavior and mechanism of collophane and dolomite separation using alkyl hydroxamic acid as a flotation collector*, Physicochemical Problems of Mineral Processing, 52(1), 155-169.

ZHOU, F., WANG, L., XU, Z., LIU, Q., CHI, R., 2015. *Reactive oily bubble technology for flotation of apatite, dolomite and quartz*, International Journal of Mineral Processing, 134, 74-81.